Nitric oxide-dependent pro-oxidant and pro-apoptotic effect of metallothioneins in HL-60 cells challenged with cupric nitrilotriacetate

Shang-Xi LIU*, Kazuaki KAWAI*, Vladimir A. TYURIN*[1], Yulia Y. TYURINA*[1], Grigory G. BORISENKO*, James P. FABISIAK*, Peter J. QUINN†, Bruce R. PITT*‡ and Valerian E. KAGAN*†‡[2]

*Department of Environmental and Occupational Health, University of Pittsburgh, 260 Kappa Drive, Pittsburgh, PA 15238, U.S.A., †Division of Life Sciences, King's College, London, U.K., and ‡Department of Pharmacology, University of Pittsburgh, Pittsburgh, PA 15238, U.S.A.

Intracellular safeguarding functions of metallothioneins (MTs) include sequestering transition and heavy metals, scavenging free radicals and protecting against electrophiles. We report that MT protection against Cu-induced cytotoxicity can be reversed and pro-oxidant and pro-apoptotic effects can be induced in HL-60 cells exposed to NO. We demonstrate that in $ZnCl_2$-pretreated HL-60 cells loaded with copper nitrilotriacetate (Cu-NTA), exposure to an NO donor, *S*-nitroso-*N*-acetyl penicillamine, resulted in S-nitrosylation and oxidation of MT cysteines. This disruption of MT Cu-binding thiolate clusters caused loosening and release of redox-active Cu, enhanced redox-cycling activity of Cu and increased peroxidation of major classes of membrane phospholipids. We also found that Cu-induced oxidative stress in $ZnCl_2$-pretreated/Cu-NTA-loaded HL-60 cells was accompanied by apoptosis documented by characteristic changes of nuclear morphology, internucleosomal DNA cleavage, externalization of phosphatidylserine, release of cytochrome *c* from mitochondria into cytosol and activation of caspase-3. We conclude that in Cu-challenged cells, NO can reverse the protective role of MTs and convert them into pro-oxidant, pro-apoptotic implements.

Key words: copper, *S*-nitroso-*N*-acetyl penicillamine, phosphatidylserine, phospholipid peroxidation, redox cycling.

INTRODUCTION

Copper is an essential metal necessary for the function of several enzymes, including cytochrome oxidase, tyrosinase and Cu/Zn-superoxide dismutase. As a transition metal, however, copper participates in Fenton-type reactions to yield several reactive oxygen species [1]. The Cu^+/Cu^{2+} redox couple can reduce oxygen to superoxide, whose dismutation produces hydrogen peroxide. The latter is further decomposed by Cu^+ to generate hydroxyl radicals capable of initiating damage to nucleic acids, proteins and lipids. Exposure of cells to excessive Cu produces cytotoxicity and induces apoptosis [2]. Thus the intracellular trafficking of Cu is tightly controlled in order to avoid its injurious redox cycling [3]. Ceruloplasmin and albumin can act as extracellular Cu-binding proteins [4,5]. Three Cu chaperones, Atx1 [6], Cox17 [7] and CCS (copper chaperone for Cu,Zn-superoxide dismutase) [8], have been characterized that safely deliver Cu to specific intracellular locations at low copper concentrations.

Metallothioneins (MTs) are low-molecular-mass (≈ 6 kDa) cysteine-rich proteins that confer resistance of cells to metal toxicity and oxidative stress. Antioxidant properties of MTs are associated with their nucleophilic SH groups acting as radical scavengers [9], but may be also realized through chelation of transition metals, such as copper, to form complexes incapable of catalysing Fenton-type reactions [10]. Paradoxically, the same thiolate clusters that are fundamentally involved in copper binding and antioxidant protection [9,10] may potentially become a source of catastrophic oxidative damage. This is because MTs readily release metals in a redox-dependent fashion. Nitrosative attack on MT cysteines has been shown to release MT-bound cadmium and enhance the cytotoxicity of this metal [11]. Furthermore, redox-driven delivery of zinc from MT to target proteins has been recently established and suggests a physiological role for MT in metal trafficking [12–14].

We have shown previously that induction of MT protected HL-60 cells against apoptosis caused by copper nitrilotriacetate (Cu-NTA) [15] and that MT binding/release of Cu can be regulated by oxidation and nitrosylation of MT cysteines *in vitro* [10,16,17]. In the current paper, we report the effects of NO on MT-mediated protection of HL-60 cells from apoptosis induced by Cu-NTA. We found that nitrosative modification of MT cysteines in Zn-pretreated/Cu-NTA-loaded HL-60 cells facilitated Cu release, elevated redox-activity of Cu and reversed the protective effect of MTs against Cu-NTA-induced apoptosis. Thus the protective ability of MT towards Cu-mediated toxicity is shifted to potentiation of cellular damage in the presence of NO.

EXPERIMENTAL

Materials and reagents

All tissue-culture media and additives were obtained from Gibco-BRL (Gaithersburg, MD, U.S.A.) except fetal bovine serum

Abbreviations used: AMC, 7-amino-4-methyl coumarin; BCS, bathocuproine sulphonate; Cu-NTA, copper nitrilotriacetate; DAF-2, 4,5-diaminofluorescein; DAF-2T, DAF-2 triazole; DTDP, 2,2′-dithiodipyridine; DTT, dithiothreitol; FBS, fetal bovine serum; GSNO, *S*-nitrosoglutathione; HMM protein, high-molecular-mass protein; MT, metallothionein; PnA, *cis*-parinaric acid; PS, phosphatidylserine; SNAP, *S*-nitroso-*N*-acetyl penicillamine.

[1] Permanent address: Institute of Evolutionary Physiology and Biochemistry, Russian Academy of Sciences, St. Petersburg, 194223 Russia.
[2] To whom correspondence should be addressed, at the Department of Environmental and Occupational Health (e-mail kagan@pitt.edu).

(FBS), which was from Sigma (St. Louis, MO, U.S.A.). Zn-MT1, $CuSO_4$, nitrilotriacetic acid disodium, 2,2′-dithiodipyridine (DTDP), *S*-nitrosoglutathione (GSNO), Ponceau S and Hoechst 33342 were also obtained from Sigma. Chloroform, methanol, hexane, propan-2-ol (HPLC grade) and Tween 20 were purchased from Aldrich Chemical Co. (Milwaukee, WI, U.S.A.). Alamar Blue was purchased from BioSource International (Sacramento, CA, U.S.A.). Proteinase K, RNase T1 and RNase A were from Roche (Indianapolis, IN, U.S.A.). Bathocuproine sulphonate (BCS; 4,7-phenylsulphonyl-2,9-dimethyl-1,10-phenanthroline) was from Fisher Scientific (Pittsburgh, PA, U.S.A.). The NO-donor *S*-nitroso-*N*-acetyl penicillamine (SNAP) was purchased from Cayman Chemical Co. (Ann Arbor, MI, U.S.A.), and concentrated stock solution was prepared freshly by dissolution in ethanol. 4,5-Diaminofluorescein (DAF-2) was purchased from CalBiochem (San Diego, CA, U.S.A.). *cis*-Parinaric acid [PnA; (9*Z*,11*E*,13*E*,15*Z*)-octadecatetraenoic acid] was obtained from Molecular Probes (Eugene, OR, U.S.A.). Monoclonal mouse antibody (E9) recognizing both MT1 and MT2 was purchased from Dako Corporation (Carpinteria, CA, U.S.A.). Mouse anti-cytochrome *c* monoclonal antibody and horseradish peroxidase-conjugated goat anti-mouse IgG specific polyclonal antibody were obtained from PharMingen International (San Diego, CA, U.S.A.). SuperSignal West Pico Chemiluminescent Substrate was purchased from Pierce (Rockford, IL, U.S.A.). Fuji X-ray film was purchased from Fisher Scientific (Pittsburgh, PA, U.S.A.). All other chemicals and regents used were of molecular-biology grade. Cu-NTA was prepared according to the method described by Toyokuni et al. [18], and the $CuSO_4$/nitrilotriacetic acid disodium molar ratio used was 1:2. The pH was adjusted to 7.4 with sodium bicarbonate.

Cell culture and treatment

HL-60 cells were grown in RPMI 1640 medium supplemented with 12% FBS at 37 °C under a 5% CO_2 atmosphere. Cells from passages 25–40 were used for the experiments. For experiments, cells (5×10^5/ml) were first treated with $ZnCl_2$ (150 μM) in medium containing 12% FBS under the same conditions as above for 24 h, and the $ZnCl_2$ was removed by centrifugation and washing with serum-free medium. The cells were re-suspended in the medium containing FBS with or without Cu-NTA (2 mM) at a density of 10^6/ml and cultured for 14 h. Cu-NTA was then removed by the above method. The cells were then treated with SNAP (100 μM) in medium containing 12% FBS at 37 °C for 4 h. SNAP was removed by repeatedly washing with PBS before the cells were utilized for various assays.

Viability assay

Cell viability was measured by quantifying the reduction of the fluorogenic indicator, Alamar Blue. Briefly, cells were re-suspended in medium containing FBS to a density of 5×10^5/ml and applied to a 96-well plate by addition of 200 μl to each well. Alamar Blue solution (20 μl) was added to each well. The cells were incubated at 37 °C for 4 h and fluorescence was determined using a Millipore Cytofluor 2350 fluorescence plate reader (Bedford, MA, U.S.A.), using excitation filter 530 ± 25 nm and emission filter 590 ± 35 nm.

Apoptosis assay by nuclear morphology

Apoptosis was assessed as described previously using Hoechst 33342 fluorescence staining [19,20]. The percentage of apoptotic cells was determined by counting the number of nuclei showing chromatin condensation and fragmentation characteristic of apoptosis after observing a total of at least 300 cells.

Low-molecular-mass DNA fragmentation in apoptotic cells

This was determined using conventional gel electrophoresis with minor modifications to our methods described previously [19,20]. Briefly, 10^6 cells were collected and washed twice with cold PBS after incubation. The pellet was suspended in 100 μl of lysis buffer (100 mM Tris/HCl, pH 8.0/1.0 mM EDTA/0.5% Triton X-100) at 4 °C for 10 min. After centrifugation, the supernatant was incubated with RNase (20 μg/ml) at 37 °C for 2 h and followed by digestion with proteinase K (100 μg/ml) at 50 °C for at least 2 h. The suspension was extracted with 20 μl of 5 M NaCl and 240 μl of alcohol at −20 °C overnight. After centrifugation, the collected DNA was electrophoresed in 2% agarose gel. Gels were stained with ethidium bromide (1 μg/ml) and evaluated under UV illumination.

Annexin V binding

Annexin V binding to cells was performed using flow cytometry essentially as described previously [19,20] with a commercially available staining kit (R & D Systems, Minneapolis, MN, U.S.A.). Briefly, after treatment, 1 ml of HL-60 cells (10^6 cells/ml) were washed twice with cold PBS. Cells were incubated with annexin V–fluorescein conjugate (1 μg/ml, final concentration) and propidium iodide (5 μg/ml) for 20 min at room temperature. Cells were analysed with a FACScan flow cytometer (Becton Dickinson) with simultaneous monitoring of green fluorescence (530 nm, 30 nm band pass filter) for annexin V–fluorescein and red fluorescence (long-pass emission filter that transmits light > 650 nm) associated with propidium iodide.

Caspase-3 activity

Caspase-3 activity in HL-60 cell lysates was measured using a fluorometric assay kit obtained from Molecular Probes (Eugene, OR, U.S.A.) essentially as described in the manufacturer's instructions. Briefly, 10^6 cells from various treatments were collected and lysed in 50 μl of ice-cold lysis buffer supplied with the kit. Then, 50 μl of 2 × substrate working solution with 10 mM dithiothreitol (DTT) and 0.2 mM fluorescent substrate, DEVD-AMC (Asp-Glu-Val-Asp-7-amino-4-methyl coumarin) conjugate, were added to each lysate and kept on ice. Samples were transferred to individual wells of a Corning 96-well plate (Acton, MA, U.S.A.) and incubated at room temperature for 30 min. Free AMC fluorescence was determined at zero time and following 30 min incubation at room temperature using a Millipore CytoFluor 2350 fluorescence plate reader, using excitation filter 360 ± 40 nm and emission filter 460 ± 40 nm. The amount of product formed was calculated using a standard curve obtained for various dilutions of AMC.

Cytochrome *c* release from mitochondria

Cells (5×10^7) from various treatments were harvested by centrifugation at 700 ***g*** for 10 min. The cell pellets were re-suspended in buffer containing 20 mM Hepes/KOH, pH 7.5, 10 mM KCl, 1.5 mM $MgCl_2$, 1.0 mM sodium EDTA, 1.0 mM sodium EGTA, 1.0 mM DTT, 0.1 mM PMSF and 250 mM sucrose [21]. The cells were homogenized with 10 strokes of a Potter–Elvehjem homogenizer and the homogenates were centrifuged at 700 ***g*** for 10 min. The supernatants were centrifuged at 100000 ***g*** for 1 h at 4 °C and the resulting pellets and supernatants were assayed for

cytochrome *c* content by Western blotting. Samples containing 10 μg of protein were resolved by SDS/PAGE (12 % gels) and transferred to 0.2 μm nitrocellulose membranes (Bio-Rad, Hercules, CA, U.S.A.). Ponceau S staining was applied to verify that equal amounts of protein were present in each lane. The membranes were blocked with 5 % non-fat milk in TBST (50 mM Tris/HCl buffer, pH 7.5, containing 200 mM NaCl, 0.05 % Tween 20) for 1 h at room temperature and subsequently probed with primary anti-cytochrome *c* antibody (1:100). Membranes were washed and then incubated with horseradish peroxidase-conjugated anti-mouse IgG secondary antibody (1:2500) for 1 h. Cytochrome *c* bands were visualized using the chemiluminescence assay system (Pierce) on Fuji X-ray film. Image capture and subsequent analysis were performed using Fluor-S Multi-Imager and Multi-Analyst software (Bio-Rad).

Separation of MTs from high-molecular-mass proteins (HMM proteins) and GSH in cell homogenates

Cells (10^8) from different treatments were washed twice with cold PBS and re-suspended in N_2-saturated potassium phosphate buffer (10 mM, pH 7.5) containing 2.0 mM EDTA and sonicated using a 4710 series Ultrasonic Homogenizer (Cole-Parmer Instrument Co., Chicago, IL, U.S.A.) for 1 min. The resulting suspension was centrifuged at 40000 ***g*** for 20 min. Supernatant was collected and applied to a Sephadex G-75 column (1 cm × 40 cm) for size-exclusion chromatography. The column was eluted with 10 mM Tris/HCl/2 mM EDTA, pH 7.8 (saturated with nitrogen), at 0.5 ml/min and 4 °C, and fractions (0.5 ml) were collected. The thiol content of each fraction was measured by adding 5 μl of DTDP solution (0.4 mM DTDP in 1.0 M sodium acetate, pH 4.0) to 20 μl of fraction solution. After 30 min incubation at room temperature, absorbance at 343 nm was recorded using a SpectroMate™ UV/VIS fibre-optic micro-spectrophotometer (World Precision Instruments, Sarasota, FL, U.S.A.) equipped with a 2 μl micropipetter cuvette.

Measurement of MTs by immuno-dot blot

MT content in the fractions was measured by immuno-dot blot with modification of the method described by Garrett et al. [22]. Purified MT1 was used as a standard. An aliquot of 0.5–10 μl from each Sephadex G-75 column fraction was diluted to 50 μl with 10 mM Tris/HCl buffer, pH 7.5, mixed with an equal volume of 3 % glutaraldehyde and then applied to nitrocellulose membrane using a Bio-Rad Bio-Dot Microfiltration Apparatus. The membrane was blocked with 5 % fat-free milk in TBST for 1 h and then incubated with mouse monoclonal anti-MT (E9) antibody for 1 h at room temperature. Non-binding primary antibody was removed by washing six times with TBST for 5 min each. The membrane was then incubated with horseradish peroxidase-conjugated polyclonal anti-mouse IgG (1:5000) in TBST for 1 h. Non-binding antibody was removed by the same washing as described above. The membrane was finally incubated with SuperSignal West Pico™ chemiluminescent substrate and exposed to X-ray film (Fuji). Image capture and subsequent analysis were performed using Fluor-S MultiImager and Multi-Analyst Software (Bio-Rad).

Fluorometric assay for *S*-nitroso-MTs

The content of S-nitrosylated cysteines in MTs was determined fluorometrically using DAF-2 as NO scavenger yielding fluorescent DAF-2 triazole (DAF-2T) [23]. The assay includes catalytic decomposition of nitrosothiol by Cu [24]. Aliquots (500 μl) of fractions of *S*-nitroso-MT obtained by Sephadex G-75 size-exclusion (as described above) were mixed with DAF-2 (5 μM) and preincubated with $CuSO_4$ (300 μM) for 2 h at 37 °C. Then, 2 ml of PBS was added to the mixture and it was centrifuged at 14000 ***g*** for 5 min. Fluorescence emission intensity of DAF-2T was determined at 515 nm with excitation at 495 nm (slits: exitation, 1.5 nm; emission, 5 nm) in a 2.5 ml cuvette using a Shimadzu RF-5301PC spectrofluorophotometer (Kyoto, Japan). The data obtained were exported and treated using RF-5301 PC Personal Software (Shimadzu). A standard curve was established by using GSNO as NO donor. The plot of GSNO concentration against DAF-2T fluorescence was linear in the concentration range from 0.04 to 0.8 μM. The content of *S*-nitroso-MT was normalized to mg of protein of HL-60 cell lysates applied to Sephadex G-75 column.

BCS/ascorbate assay of 'loosely bound' and total Cu in chromatographic fractions of HL-60 cell lysates

Lysates were prepared from HL-60 cells by suspending 10^8 cells in 1 ml of 10 mM Tris/HCl buffer, pH 7.4, and sonicating them for 1 min using a 4710 series Ultrasonic Homogenizer. The resulting suspension was centrifuged at 40000 ***g*** for 20 min. The cleared lysate was applied to a Sephadex G-75 column. Fractions corresponding to HMM proteins, MT and GSH were identified by DTDP assay of thiols and immuno-dot blot assay and pooled separately. These pooled fractions (≈ 5 ml) were evaporated using a SpeedVac™ (Savant Instruments, Farmingdale, NY, U.S.A.) and concentrated 15-fold. The resulting samples were added to BCS (100 μM) and ascorbate (400 μM) solution in 10 mM Tris/HCl buffer, pH 7.4. The amount of Cu available for BCS chelation was evaluated by measuring the absorbance of the BCS–Cu(I) complex using the molar absorbance coefficient of 13500 $M^{-1} \cdot cm^{-1}$ at 480 nm [25] using a SpectroMate™ UV/VIS fibre-optic micro spectrophotometer with capillary microcuvette (15 μl sample volume and 10 cm optical path length). 'Loosely bound' Cu was defined as the amount accessible to BCS binding after 30 min of incubation at room temperature with BCS and ascorbate. Total Cu was taken as the amount of Cu–BCS complex formed after complete oxidation of thiols in the sample by 20 min treatment with H_2O_2 (10 mM). Addition of catalase (80 units/ml) was used to stop the oxidative reaction prior to measurement of Cu–BCS absorbance.

EPR assay of ascorbate radicals

Ascorbate (60 μM) was added to homogenate of HL-60 cells (5×10^6 cells) in 60 μl of 50 mM disodium phosphate buffer, pH 7.4, and EPR spectra of ascorbate radicals were recorded immediately. EPR measurements were performed on a JEOL-RE1X spectrometer (Tokyo, Japan) at 25 °C using gas-permeable Teflon tubing (0.8 mm internal diameter, 0.013 mm thickness) obtained from the Alpha Wire Corporation (Elizabeth, NJ, U.S.A.). The tube (≈ 8 cm in length) was filled with 60 μl of mixed sample, folded into quarters and placed in an open 3 mm internal-diameter EPR quartz tube so that the entire sample was within the effective microwave area. Spectra of ascorbate radicals were recorded at: 335.5 mT, centre field; 20 mW, power; 0.05 mT, field modulation; 5 mT, sweep width; 4000, receiver gain; 0.1 s, time constant.

Assay of phospholipid peroxidation in HL-60 cells

PnA was incorporated into $ZnCl_2$-pretreated and $ZnCl_2$-pretreated/Cu-NTA-loaded HL-60 cells (10^6 cells/ml) by addition

of PnA–human serum albumin complex to give a final concentration of 2.0 μg of PnA/10^6 cells in serum-free RPMI 1640 medium without Phenol Red as described earlier [26]. PnA-labelled cells were treated with SNAP (100 μM) for 4 h at 37 °C in RPMI 1640 medium with 10 % FBS. At the end of incubation period, cells were centrifuged, washed twice with PBS and total lipids were extracted using the Folch procedure [27] in the presence of butylated hydroxytoluene to retard subsequent oxidation. The lipid extract was dried under N_2, dissolved in 0.2 ml of propan-2-ol/hexane/water (4:3:0.16, by vol.) and separated by normal-phase HPLC using a 5 μm Microsorb-MV™ Si column (4.6 × 250 mm) and an ammonium acetate gradient as described earlier [26]. The separations were performed using a Shimadzu HPLC system (LC-600) equipped with an in-line RF-551 fluorescence detector. Fluorescence of PnA was measured at 420 nm emission after excitation at 324 nm. Data were processed and stored in digital form with Shimadzu EZChrom software. Lipid phosphorus was determined using a micro method [28].

Determination of protein

Protein concentration in the HL-60 cell homogenates was determined with the Bio-Rad Protein Assay kit using BSA as a standard.

Statistical analysis

The results are presented as means ± S.E.M. from at least three experiments and statistical analysis was performed by paired Student's *t* test or one-way ANOVA. The statistical significance of differences was set at $P < 0.05$.

RESULTS

NO-induced apoptosis in $ZnCl_2$-pretreated/Cu-NTA-loaded HL-60 cells

We demonstrated previously that pretreatment of HL-60 cells with $ZnCl_2$ protected cells from apoptosis induced by Cu-NTA due to sequestration of intracellular Cu by MTs and elimination of redox-cycling activity of Cu [15]. We wondered whether NO, which is able to release Cu from Cu-MT in cell-free biochemical systems, could also release Cu from Cu-MT in cells and reverse the protective effect of MT. To this end, HL-60 cells were first pretreated with 150 μM $ZnCl_2$ for 24 h to induce MT as described previously [15]. Cells were then incubated with 2 mM Cu-NTA for 14 h. Previous results showed that exposure of naïve HL-60 cells (non-pretreated with $ZnCl_2$) to Cu-NTA at this concentration caused more than a 90 % decrease of viability, but had almost no effect on $ZnCl_2$-pretreated cells [15]. After removing excess Cu-NTA, the cells were incubated with 100 μM SNAP at 37 °C for 4 h.

We first utilized Alamar Blue to determine if SNAP induced any changes in cell viability after the 4 h exposure. Naïve and $ZnCl_2$-pretreated cells in the absence of Cu-NTA treatment exposed to SNAP were 98.6 and 97.9 % viable, respectively, compared with their non-SNAP-treated counterparts. Surprisingly, exposure of $ZnCl_2$-pretreated Cu-NTA-loaded cells to SNAP produced a small but significant change in viability, as measured by Alamar Blue (94.5 % relative to non-SNAP-treated counterparts). Since a 4 h exposure to SNAP might not be sufficient to produce gross changes in cell viability characteristic of necrosis or late apoptosis, we also assessed specific biomarkers of early apoptosis. These included changes of nuclear morphology, internucleosomal DNA fragmentation and externalization of phosphatidylserine (PS), as well as cytochrome *c* release from mitochondria and activation of caspase-3.

Nuclear morphology

Chromatin condensation and fragmentation are characteristics of apoptotic cells. Table 1 shows the percentage of cells with apoptotic nuclear morphology visualized by Hoechst 33342 in the absence and presence of SNAP treatment. It is clear that SNAP itself produced no change in nuclear morphology in naïve cells. On the other hand, for $ZnCl_2$-pretreated/Cu-NTA-loaded cells the percentage of apoptotic cells rose to 35 % after SNAP exposure. SNAP produced only a minor increase in apoptosis in $ZnCl_2$-pretreated cells not exposed to Cu, with less than 10 % of cells showing apoptotic nuclei. Importantly, pro-apoptotic effects of SNAP in $ZnCl_2$-pretreated/Cu-NTA-loaded cells could be prevented completely by the Cu chelator, neocuproine (Table 1).

DNA fragmentation

Analysis of DNA fragmentation, another hallmark of apoptosis, was also conducted. Figure 1 shows the formation of DNA ladders characteristic of internucleosomal DNA cleavage with and without SNAP treatment. Naïve (lanes 1 and 2) and $ZnCl_2$-pretreated (lanes 3 and 4) cells showed essentially no DNA fragmentation in both SNAP-treated (lanes 2 and 4) and non-SNAP-treated (lanes 1 and 3) cells. In contrast, in cells pretreated

Table 1 SNAP-induced changes in nuclear morphology, annexin V binding and caspase-3 activity in HL-60 cells

Cells (5×10^5/ml) were incubated in RPMI 1640 medium containing 12% FBS and 150 μM $ZnCl_2$ for 24 h to induce MT synthesis. $ZnCl_2$ was subsequently removed by washing with serum-free RPMI 1640. A portion of $ZnCl_2$-treated cells (10^6/ml) was loaded with Cu by resuspending in RPMI 1640 containing 12% FBS and 2 mM Cu-NTA and cultured for an additional 14 h. Naïve (non-$ZnCl_2$-treated) and $ZnCl_2$-pretreated cells were cultured similarly in the absence of Cu-NTA. Some $ZnCl_2$-pretreated/Cu-NTA-loaded cells were also preincubated with neocuproine (100 μM) at 37 °C for 1 h prior to the addition of SNAP. Cells were then washed with serum-free medium and resuspended in medium containing 12% FBS with or without 100 μM SNAP and incubated for 4 h at 37 °C. Apoptotic nuclear morphology, annexin V binding and capase-3 activity were measured as described in the Experimental section. Results on annexin V binding are presented as the percentage of annexin V-positive (+)/propidium iodide-negative (−) cells. Data are means ± S.E.M. from three replicated experiments. *$P < 0.01$, †$P < 0.05$ against $ZnCl_2$-pretreated/Cu-NTA-loaded HL-60 cells that were not exposed to SNAP; ‡$P < 0.01$ against $ZnCl_2$-pretreated/Cu-NTA-loaded HL-60 cells exposed to SNAP. FI, fluorescence intensity.

	Apoptotic nuclear morphology (% apoptotic cells)			Annexin V binding [% annexin V (+)/propidium iodide (−) cells]		Caspase-3 activity (FI/mg of protein per min)	
	−SNAP	+SNAP	+SNAP + neocuproine	−SNAP	+SNAP	−SNAP	+SNAP
Naïve	4.7 ± 0.5	5.1 ± 0.5	–	3.2 ± 0.6	3.9 ± 0.8	121 ± 11	113 ± 19
Zn	5.1 ± 0.3	9.0 ± 1.2	–	2.9 ± 1.4	5.3 ± 0.4	133 ± 34	203 ± 31
Zn/Cu-NTA	5.5 ± 0.3	36.8 ± 2.7*	8.8 ± 1.2‡	3.6 ± 1.7	22.5 ± 1.7*	128 ± 36	803 ± 33†

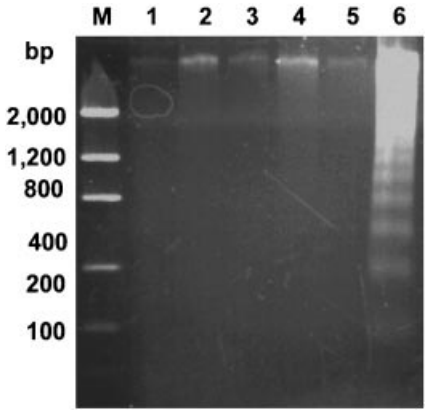

Figure 1 SNAP induces internucleosomal DNA cleavage only in $ZnCl_2$-pretreated/Cu-NTA-loaded HL-60 cells

Cell suspensions (5×10^5/ml) were incubated in RPMI 1640 medium containing 12% FBS and 150 μM $ZnCl_2$ for 24 h to induce MT synthesis. $ZnCl_2$ was subsequently removed by washing with serum-free RPMI 1640. Aliquots of the $ZnCl_2$-treated cells (10^6/ml) were then loaded with Cu by re-suspending in RPMI 1640 with 12% FBS/2 mM Cu-NTA and cultured for an additional 14 h. Naïve (non-$ZnCl_2$-treated cells) and $ZnCl_2$-pretreated cells were similarly cultured in the absence of Cu-NTA. Cells then were washed with serum-free medium and re-suspended in medium containing 12% FBS with or without 100 μM SNAP and incubated for 4 h at 37 °C. At the end of incubation cells were washed twice with cold PBS and DNA was extracted and subjected to gel electrophoresis as described in the Experimental section. Lane M, DNA molecular mass markers. Lanes 1–6 represent naïve (lanes 1 and 2), $ZnCl_2$-pretreated (lanes 3 and 4) and $ZnCl_2$-pretreated/Cu-NTA-loaded (lanes 5 and 6) HL-60 cells in the absence (lanes 1, 3 and 5) and presence (lanes 2, 4 and 6) of SNAP (100 μM, 4 h).

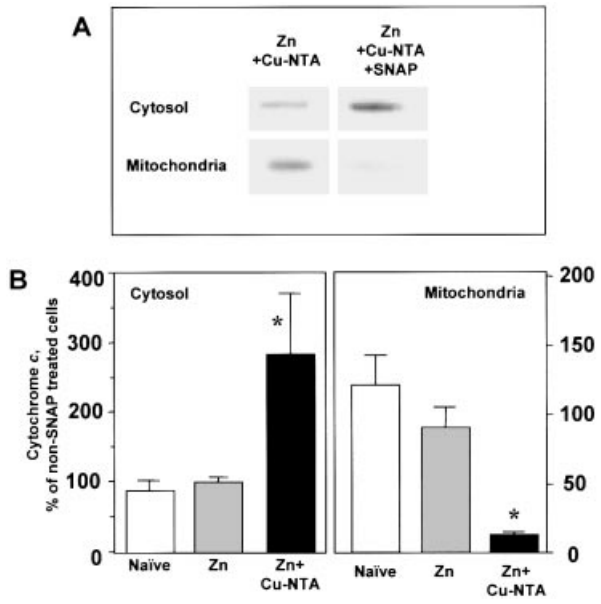

Figure 2 Release of cytochrome *c* from mitochondria into the cytosol in $ZnCl_2$-pretreated/Cu-NTA-loaded HL-60 cells after exposure to SNAP

Cells were treated as described in Figure 1. Cytochrome *c* content in mitochondria and cytosol were measured by Western blotting as described in the Experimental section. (**A**) A typical Western blot of cytochrome *c* protein in both cytosolic and mitochondrial fractions obtained from $ZnCl_2$-pretreated/Cu-NTA-loaded cells with and without SNAP treatment. Following SNAP exposure there was a clear decrement in the mitochondrial content of cytochrome *c* simultaneous with its increased appearance in the cytosol. (**B**) Quantification of absorbance for the cytosolic and mitochondrial cytochrome *c* signals obtained using a Bio-Rad Fluor-S MultiImager and Multi-Analyst software. Data are means ± S.E.M. from three independent experiments. $^*P < 0.05$ against naïve and $ZnCl_2$-pretreated cells.

with $ZnCl_2$ and loaded with Cu-NTA (lanes 5 and 6), 180–200 bp DNA 'ladders' were readily apparent only after SNAP treatment (lane 6); no detectable internucleosomal DNA cleavage appeared without SNAP treatment (lane 5).

PS externalization

PS externalization is one of the earliest events in apoptosis. We next measured the extent of PS externalization following SNAP treatment using fluorescently labelled annexin V and flow cytometry. Table 1 shows the percentage of annexin V-positive/propidium iodide-negative cells following SNAP treatment. Percentage of cells showing PS externalization in naïve and $ZnCl_2$-pretreated cells was low (< 5%) in the absence of SNAP and did not change significantly after SNAP treatment. SNAP treatment of $ZnCl_2$-pretreated Cu-NTA-loaded cells, however, resulted in a significant rise in annexin V-positive/propidium iodide-negative cells up to 23%.

Cytochrome *c* release from mitochondria

Recent studies showed that cytochrome *c* is released from mitochondria into the cytosol during apoptosis, and participates in the formation of apoptosomes and activation of caspases [29–31]. Therefore, we next measured cytochrome *c* content in mitochondria and cytosol in HL-60 cells after incubation with SNAP using Western blotting. Figure 2(A) shows a typical Western blot of cytochrome *c* in mitochondria and cytosol after SNAP treatment in $ZnCl_2$-pretreated/Cu-NTA-loaded cells. In these cells, SNAP caused an observable increase in the cytosolic content of cytochrome *c* and a similar decrease in mitochondrial cytochrome *c* as compared with non-SNAP-treated cells. Quantification of these data expressed relative to non-SNAP-treated cells is shown in Figure 2(B). SNAP induced a 3-fold increase in cytosolic cytochrome *c* and a similar decrement (> 4-fold decrease) in mitochondrial cytochrome *c* content. No significant changes in cytochrome *c* distribution were found after exposure of naïve and $ZnCl_2$-pretreated cells to SNAP.

Activation of caspase-3

Next we determined activity of caspase-3 in HL-60 cells under different conditions. Table 1 shows changes in caspase-3 activity after SNAP treatment. There were no significant changes in caspase-3 activity in either naïve or $ZnCl_2$-pretreated HL-60 cells after SNAP exposure. In contrast, a more than 6-fold activation of caspase-3 activity was observed in $ZnCl_2$-pretreated/Cu-NTA-loaded cells after SNAP treatment.

Effect of SNAP on MT SH groups in HL-60 cells

MTs contain 20 cysteines, which can be oxidized or nitrosylated in the presence of NO donors [11,17]. Therefore, we next investigated the redox state of SH groups in MTs after SNAP treatment. We separated MTs from HMM proteins and GSH in cell homogenates by Sephadex G-75 size-exclusion under very strict nitrogen-saturated conditions. The content of reduced thiols in each fraction was measured by DTDP assay. Figure 3 shows Sephadex G-75 profiles of thiol distribution of cells pretreated with $ZnCl_2$ (Figure 3A) or with both $ZnCl_2$ and Cu-NTA (Figure 3B) in the absence and presence of SNAP. As we

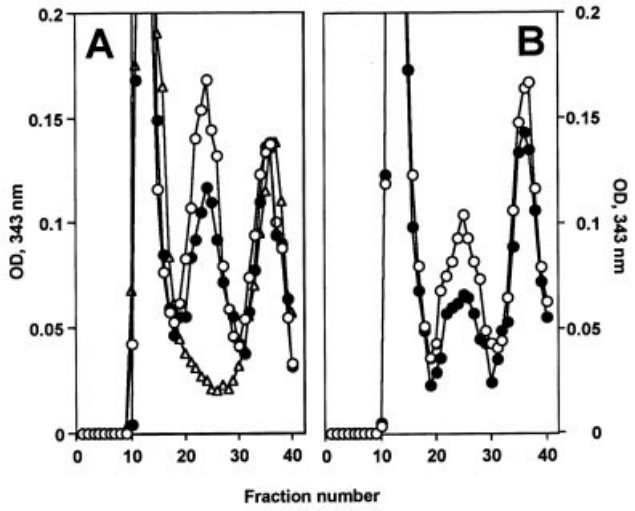

Figure 3 Sephadex G-75 chromatographic profiles of the thiol distribution from (A) $ZnCl_2$-pretreated cells and (B) $ZnCl_2$-pretreated/Cu-NTA-loaded cells

Cell treatment was as described in Figure 1. Cells (10^8) from each treatment were then washed with cold PBS and cytosolic fractions were prepared and analysed for SH content using DTDP as described in the Experimental section. ○, $ZnCl_2$-pretreated cells; ●, $ZnCl_2$-pretreated/Cu-NTA-loaded cells; △, naïve cells.

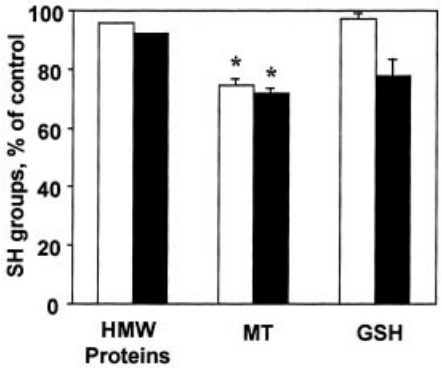

Figure 4 Changes of thiol content in HMM protein, MT and GSH fractions in $ZnCl_2$-pretreated and $ZnCl_2$-pretreated/Cu-NTA-loaded HL-60 cells after exposure to SNAP

Cell treatment was as described in Figure 1. Chromatographic conditions were identical to those in Figure 3. Fractions from HMM protein, MT and GSH peaks were pooled (0.5 ml × 10 = 5 ml) and thiols were measured using DTDP assay. Results are expressed as the percentage of thiols in non-SNAP-treated cells (100%) and shown as means ± S.E.M. ($n = 3$). Open bars, $ZnCl_2$-pretreated cells; closed bars, $ZnCl_2$-pretreated/Cu-NTA-loaded cells. $^*P < 0.05$ against non-SNAP-treated cells.

reported in a previous paper [15], the SH profile contains three different peaks: the HMM protein peak, containing relatively large amounts of thiol groups, the middle MT peak, as proved by immuno-dot blotting, and the low-molecular-mass peak containing GSH. The MT peak was essentially not detected in naïve control cells (Figure 3A, △). We have previously observed that Zn pretreatment results in at least a 50-fold induction of MT compared with naïve cells [15]. After SNAP exposure, SH groups in protein and GSH in $ZnCl_2$-pretreated cells essentially did not change but that in MT decreased significantly (Figure 3A). In cells pretreated with both $ZnCl_2$ and Cu-NTA, thiols similarly decreased in MTs (Figure 3B). It should be noted that the measurement of thiols in MTs obtained from Cu-treated cells may be an underestimation based on the fact that Cu is not easily displaced from MTs even at low pH and, hence, residual Cu may mask some thiols from reaction with DTDP. A slight decrease in reduced SH was apparent in GSH. We then pooled fractions from each peak and measured the total SH content within the peak. Compared with non-SNAP-exposed cells, SH groups in MTs had a significant decrease in both $ZnCl_2$-pretreated cells (26% decrease) as well as in $ZnCl_2$-pretreated/Cu-NTA-loaded cells (28% decrease). The decrease of reduced GSH was not significant (Figure 4).

Using slot-blot assays we determined the contents of MTs in the MT fractions obtained from $ZnCl_2$-pretreated cells as well as from $ZnCl_2$-pretreated SNAP-exposed cells and found them to be 1.2 and 1.1 nmol/mg of protein, respectively. Based on this we were able to estimate on a molar basis that changes in MT SH groups in $ZnCl_2$-pretreated cells decreased from 21 to 15 mol of SH/mol of MT after SNAP exposure. We were not able to obtain the accurate changes in molar ratios of SH/MT in HL-60 cells pretreated with both $ZnCl_2$ and Cu-NTA, because the E9 monoclonal antibody used does not appear to recognize Cu-MT. If we assume no change in the level of MT protein following Cu loading then the changes in MT SH groups will be similar to those in cells pretreated with $ZnCl_2$ alone.

Nitrosylation of MTs in HL-60 cells exposed to SNAP

Nitrosative attack on MTs in HL-60 cells may result in their S-nitrosylation. The nitrosylated thiols may be relatively stable or undergo denitrosylation. To estimate the level of MT S-nitrosylation after exposure of cells to SNAP we used a specific fluorogenic reagent for NO that may be released from S-nitrosothiols upon exposure to Cu^+. Figure 5 shows that exposure to SNAP significantly increased the amount of S-nitrosylated MTs in both $ZnCl_2$-pretreated cells and $ZnCl_2$-pretreated/Cu-

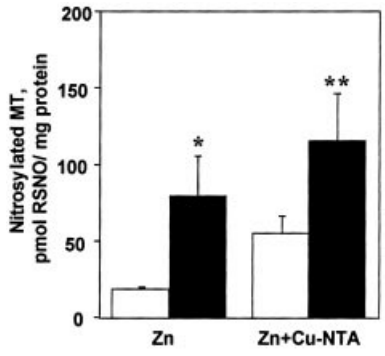

Figure 5 Content of *S*-nitroso-MT in $ZnCl_2$-pretreated and $ZnCl_2$-pretreated/Cu-NTA-loaded HL-60 cells after exposure to the NO donor, SNAP

The content of S-nitrosylated cysteines (RNSOs) in MTs was determined fluorometrically using DAF-2 as a NO scavenger yielding fluorescent DAF-2T after catalytic decomposition of nitrosothiols by Cu. Closed bars, after exposure to SNAP; open bars, in the absence of SNAP. Data are means ± S.E.M., $n = 6$. $^*P < 0.02$, $^{**}P < 0.005$ against $ZnCl_2$-pretreated cells.

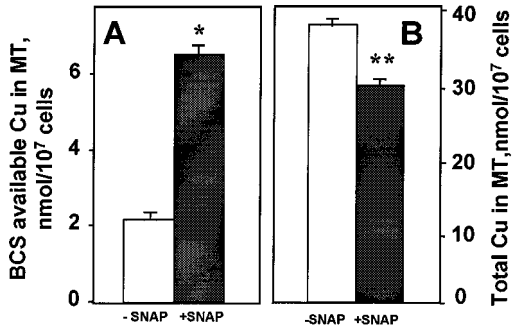

Figure 6 Content of loosely bound and total Cu in MTs from $ZnCl_2$-pretreated and $ZnCl_2$-pretreated/Cu-NTA-loaded cells in the presence and absence of SNAP

$ZnCl_2$-pretreated and $ZnCl_2$-pretreated/Cu-NTA-loaded HL-60 cells were exposed to SNAP for 4 h and lysates prepared and subjected to Sephadex G-75 chromatography. Loosely bound (**A**) and total (**B**) Cu in MT fractions were detected by optical spectroscopy of BCS–Cu(I) complexes, as described in the Experimental section. Data are means ± S.E.M., $n = 3$. $^{*}P < 0.01$, $^{**}P < 0.05$ against the respective non-SNAP-treated cells.

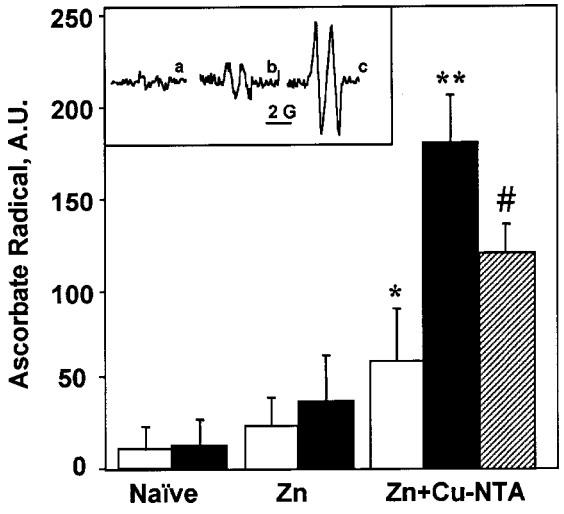

Figure 7 Redox-cycling activity of Cu assessed by EPR measurements of ascorbate radical production in homogenates from HL-60 cells in the absence and presence of SNAP

The inset shows typical EPR spectra of ascorbate radicals in naïve cells (trace a), $ZnCl_2$-pretreated/Cu-NTA-loaded cells (trace b) and $ZnCl_2$-pretreated/Cu-NTA-loaded cells exposed to SNAP (trace c). The Figure shows the average magnitude of ascorbate radical signal measured over 8 min after addition of ascorbate (60 μM). Closed bars, after exposure to SNAP; open bars, in the absence of SNAP; hatched bar, addition of neocuproine (100 μM, 1 h) before exposure to SNAP. Data are means ± S.E.M., $n = 3$. $^{*}P < 0.05$ against naïve cells; $^{**}P < 0.005$ against naïve and non-SNAP-treated, $ZnCl_2$-pretreated/Cu-NTA-loaded cells; $^{\#}P < 0.05$ against SNAP-treated, $ZnCl_2$-pretreated/Cu-NTA-loaded cells.

NTA-loaded cells. There was no significant difference in the amounts of *S*-nitroso-MT between $ZnCl_2$-pretreated cells and $ZnCl_2$-pretreated/Cu-NTA-loaded cells after SNAP. Based on our slot-blot estimates of MT content only a very small fraction ($< 0.3\,\%$) of MT was retained as *S*-nitroso-MT after a 4 h exposure to SNAP. Thus SNAP-induced S-nitrosylation of MTs in HL-60 cells occurred transiently and their denitrosylation probably resulted in oxidative loss of SH groups. To estimate the role of thiol oxidation in MTs after exposure of HL-60 cells to SNAP we used DTT to evaluate the fraction of recoverable MT cysteines. We found that about $30\,\%$ of the thiols lost after exposure to SNAP were recovered after treatment with DTT (2 mM, 30 min) in both $ZnCl_2$-treated and $ZnCl_2$-treated/Cu-NTA-loaded HL-60 cells. Thus $\approx 70\,\%$ of the lost thiols in MT were modified beyond oxidation to disulphides and/or mixed sulphides (possibly to sulphinic and sulphonic acids [32,33]) after exposure to SNAP and could not be reduced by DTT.

Effect of SNAP on sequestration of Cu by MT in HL-60 cells

Our previous results showed that Cu was mainly accumulated in MTs in $ZnCl_2$-pretreated cells after exposure to Cu-NTA [15]. Additionally, we demonstrated that Cu could be released from MT by nitrosative attack on MT cysteines using experiments *in vitro* [17]. With this in mind, we next measured the changes of Cu sequestration in MT after SNAP treatment of $ZnCl_2$-pretreated/Cu-NTA-loaded cells. Figure 6 shows that the amount of loosely bound Cu (available for BCS-binding) in the MT fraction increased by about 3-fold after SNAP treatment (Figure 6A). Total Cu in the MT fraction decreased by $\approx 20\,\%$ after SNAP exposure (Figure 6B), suggesting that Cu had been released as a result of MT–NO interaction. This released Cu from MT was partly recovered in the GSH peak (results not shown).

Effect of SNAP on redox-cycling activity of Cu in HL-60 cells

Since the cytotoxic effects of Cu are associated, to a large extent, with its ability to generate reactive oxygen species [1], we next investigated the redox-cycling activity of Cu in HL-60 cells exposed to SNAP. For this, we employed sensitive and specific EPR measurements of Cu-dependent ascorbate radical production in cell homogenates upon addition of exogenous ascorbate. Figure 7 shows the typical EPR spectra (insets) and magnitudes of ascorbate radical EPR signals produced by HL-60 cell homogenates in the absence of SNAP and after exposure of cells to SNAP. Barely detectable EPR signals of ascorbate radicals were obtained from homogenates prepared from naïve or $ZnCl_2$-pretreated cells (Figure 7, inset, a), indicative of the absence of Cu in these cells. Exposure to SNAP did not produce any significant changes in the magnitude of the signals. In $ZnCl_2$-pretreated/Cu-NTA-loaded HL-60 cells, however, a significantly greater ascorbate radical EPR signal was observed (Figure 7, inset, b) whose magnitude was increased more than 3-fold in cells exposed to SNAP (Figure 7, inset, c). Thus SNAP caused a dramatic increase in redox-cycling activity of Cu in the $ZnCl_2$-pretreated/Cu-NTA-loaded cells. We further studied the effects of a Cu^{+} chelator, neocuproine, on redox-cycling activity of copper in $ZnCl_2$-treated/Cu-NTA-loaded HL-60 cells exposed to SNAP. We found that neocuproine was able to significantly protect against SNAP-induced ascorbate radical production. In the presence of neocuproine, the magnitude of ascorbate radical signals (steady-state concentrations of ascorbate radicals) was not significantly different from that in $ZnCl_2$-treated/Cu-NTA-loaded HL-60 cells that were not exposed to SNAP (Figure 7).

Effect of SNAP on oxidation of PnA-labelled phospholipids in HL-60 cells

Elevated redox-cycling activity of Cu released by SNAP may cause oxidative stress in cells [15]. To determine whether SNAP exposure induced oxidative stress in membrane phospholipids of HL-60 cells we utilized our sensitive HPLC fluorescent technique. We metabolically trans-acylated cell phospholipids with a natural fluorescent fatty acid, PnA, containing four conjugated double bonds. The presence of the conjugated double-bond system is

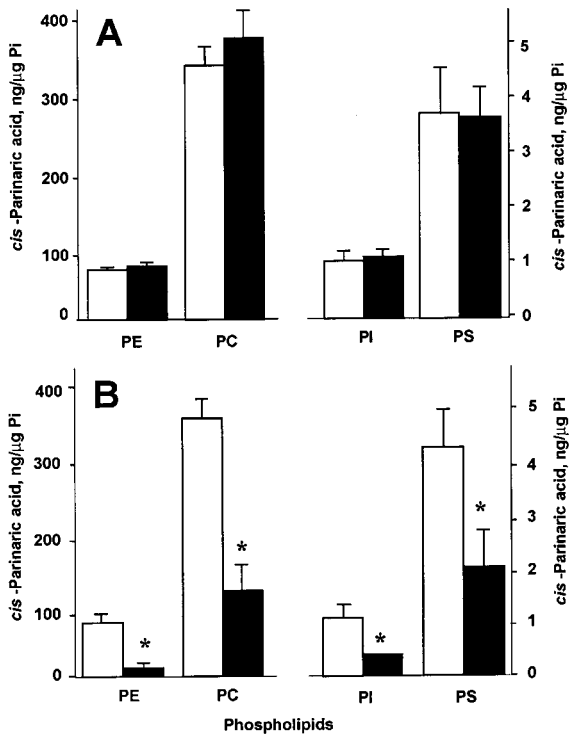

Figure 8 Effect of SNAP on oxidation of PnA-labelled phospholipids in naïve, $ZnCl_2$-pretreated and $ZnCl_2$-pretreated Cu-NTA-loaded HL-60 cells

Naïve (**A**), $ZnCl_2$-pretreated and $ZnCl_2$-pretreated/Cu-NTA-loaded (**B**) HL-60 cells were metabolically labelled with PnA as described in the Experimental section. PnA-labelled cells were then exposed to SNAP for 4 h at 37 °C. At the end of incubation, cells were spun down, washed twice with PBS and lipids were extracted and resolved by HPLC. PI, phosphatidylinositol; PE, phosphatidylethanolamine; PC, phosphatidylcholine. Data are means ± S.E.M., $n = 3$. (**A**) Open bars, naïve HL-60 cells not exposed to SNAP; closed bars, naïve HL-60 cells exposed to SNAP. (**B**) Open bars, $ZnCl_2$-pretreated cells exposed to SNAP; closed bars, $ZnCl_2$-pretreated/Cu-NTA-loaded cells exposed to SNAP. $^*P < 0.05$ against $ZnCl_2$-pretreated SNAP-exposed cells.

responsible for its fluorescence and confers high sensitivity to oxidative stress [26]. Disruption of the conjugated double-bond system by oxidation results in loss of fluorescence from specific classes of labelled phospholipids. Since mammalian cells do not synthesize conjugated double systems the fluorescence loss is irreparable and can be used for quantitative analysis of oxidative stress in thus-labelled cells [26]. Figure 8(B) shows that the content of PnA-labelled oxidation-sensitive phospholipids was substantially higher in $ZnCl_2$-pretreated cells exposed to SNAP than in $ZnCl_2$-pretreated/Cu-NTA-loaded cells exposed to SNAP. A more than 2-fold decrease of PnA contained in four major classes of membrane phospholipids (phosphatidylcholine, phosphatidylethanolamine, PS and phosphatidylinositol) was caused by SNAP in $ZnCl_2$-pretreated/Cu-NTA-loaded HL-60 cells as compared with $ZnCl_2$-pretreated cells. No significant changes in the content of PnA-labelled phospholipids were detected upon exposure of naïve cells to SNAP (Figure 8A).

DISCUSSION

MT is a cysteine-rich protein in which binding of metals occurs through their co-ordination in thiolate clusters [34–36]. Therefore, the effectiveness of metal sequestration by MTs is strictly dependent on the oxidative state of their SH groups. Both oxidative and nitrosative attacks on MT cysteines have been shown to liberate MT-bound metals (Zn, Cd, Cu) in cell-free model systems [10–14,17,37]. Moreover, recent work demonstrated that Zn could be undirectionally transferred from Zn-MT to a number of target proteins with lower affinities for the metal after redox modification of MT cysteines [12–14]. Similarly, we found that NO was able to induce transfer of Cu from Cu-MT to apo/Zn-superoxide dismutase, to reconstitute superoxide dismutase activity without concomitant redox-cycling activity of copper [17].

While these *in vitro* demonstrations clearly indicate that there is a possibility for redox regulation of metal occupancy in MTs and for the transfer of metals to other target proteins it remains to be elucidated whether this mechanism may be effectively realized in intracellular environments *in vivo*. Misra et al. [11] reported that Cd could be released from MTs in CHO-K1 Chinese hamster ovary cells exposed to NO donors. We reported recently that NO was capable of causing a conformational change in a MT chimaera measured via fluorescence resonance energy transfer that was consistent with release of metals from MT [38]. It is not clear whether NO can similarly change the redox state of Cu-MT in cells and, if so, what the consequences are. Being a redox-active metal, Cu can facilitate both nitrosylation and denitrosylation of protein cysteines and *S*-nitrosocysteine, respectively [39,40]. In this paper, we demonstrate for the first time that NO is able to release Cu from Cu-MT and induce Cu-dependent oxidative stress in HL-60 cells.

NO reverses the protective effect of MT against apoptosis induced by Cu-NTA

As we reported previously induction of MT protected HL-60 cells from apoptosis caused by Cu-NTA [15]. When we treated these Zn-induced/Cu-loaded cells with a NO donor, SNAP, at non-toxic concentrations (100 μM), the protective effect was reversed and apoptosis readily occurred, as measured by multiple early and late markers. NO alone did not induce apoptosis at the concentration used in this experiment since no cytotoxic effects were observed in the absence of Cu-NTA treatment. Since our previous work demonstrated that Cu was sequestered almost exclusively in MTs in HL-60 cells challenged with Cu-NTA [15], we hypothesized that NO reverses the protective function of MTs and converts them into a cytotoxic pro-apoptotic implement under conditions of Cu load. Therefore, we were extremely interested in understanding the mechanisms involved in pro-apoptotic interactions of NO with Cu-MTs.

SNAP induces redox modification of MT in HL-60 cells, releases redox-active Cu and induces oxidative stress in HL-60 cells

We hypothesized that NO attack on MT cysteines would result in their nitrosative/oxidative modification, hence weakening the affinity of MT for bound Cu. This would facilitate redox-cycling activity of Cu, yielding oxidative stress and triggering the apoptotic machinery. We performed experiments to test all essential stages of this pathway. Indeed, we were able to demonstrate that exposure to SNAP was responsible for the loss of five out of 21 SH groups/MT molecule in HL-60 cells. Thus NO was able to effectively interact with MT cysteines in HL-60 cells despite its reported relatively low reactivity towards MT cysteines under anaerobic conditions *in vitro* [41]. Presumably, sufficient oxygen was available under these conditions to allow the complex NO–SH interactions to occur. We found no significant differences in the SNAP-induced loss of MT cysteines between $ZnCl_2$-pretreated cells or $ZnCl_2$-pretreated/Cu-NTA-loaded cells, suggesting that Cu was not crucial for redox modification of MT cysteines by NO. This implies that NO-

driven redox modification of MT cysteines may act as a universal mechanism through which nitrosative signalling can regulate the ability of MT to sequester and/or dispense metal ions.

We also observed that MT appeared more sensitive to thiol loss than the HMM protein fraction or GSH. Similar preference for MT SH-group oxidation was observed by Quesada et al. [42] following exposure of Zn-induced HL-60 cells to H_2O_2. This could arise if MT thiols are particularly more sensitive to nitrosation/oxidation than the SH groups contained in other proteins or GSH. Alternatively, it may reflect differences in the capacity for protein repair and regeneration of reduced SH groups. While mechanisms describing the thioredoxin/glutaredoxin-dependent regeneration of oxidized cysteines of GSH and various proteins has been well described [43,44], essentially little is known regarding the specific regenerative capacity of MT cysteines.

We further established that only a relatively small fraction ($\approx$ 2–3 %) of oxidatively modified MT cysteines were retained as *S*-nitroso-MT in cells under the conditions of our assay. This suggests that significant denitrosylation of *S*-(Cys)-nitroso-MT occurred under the conditions of our assay; however, the subsequent products of this reaction were still manifest as modified thiols (loss of reduced SH groups). Our experiments with DTT demonstrated that only about 30 % of MT cysteines lost after exposure to SNAP were recoverable in both $ZnCl_2$-treated and $ZnCl_2$-treated/Cu-NTA-loaded HL-60 cells. Therefore, a significant number of the cysteines in MT underwent oxidation beyond disulphides or mixed sulphides to probably form sulphinic and sulphonic acids. These results suggest that oxidation of thiols to disulphides and mixed sulphides and their further oxidative modification to sulphinic and sulphonic acids should be considered when the effects of NO and NO donors on critical thiol-containing proteins are investigated [32,33]. The fractions of *S*-(Cys)-nitroso-MT were almost the same in both $ZnCl_2$-pretreated cells and $ZnCl_2$-pretreated/Cu-NTA-loaded cells, again indicating that Cu was probably not involved in denitrosylation of *S*-nitroso-MTs. If such reactions occur *in vivo* they are undoubtedly complex and multi-faceted and reflect the need for biochemical mechanisms necessary for regeneration of reduced cysteines to preserve the metal-binding capacity of MT. We have previously observed that dihydrolipic acid, a naturally occurring thiol antioxidant, can regenerate reduced thiols in MT previously exposed to H_2O_2 or NO and restore its metal-binding ability [16].

In line with several *in vitro* observations on release of metals from oxidatively/nitrosatively modified MTs we found that the MT fraction obtained from $ZnCl_2$-pretreated/Cu-NTA-loaded HL-60 cells had significant alterations in bound Cu after exposure to SNAP. First, SNAP liberated a portion of the Cu bound to MT ($\approx$ 22 % of total Cu in Cu-MTs) to produce a pool of free copper no longer detectable in the MT fraction (but partly recoverable in the GSH fraction). Secondly, it 'loosened' a significant part of MT-bound Cu to such an extent that $\approx$ 15–20 % of the Cu contained within the MT fraction became available for BCS chelation. Based on previous results on redox-cycling activity of free and loosely bound Cu *in vitro* [17], one would expect that there would be a substantially enhanced redox-cycling activity of Cu after exposure of HL-60 cells to SNAP. Indeed, SNAP caused a 3-fold increase in the rate of ascorbate radical formation in homogenates from $ZnCl_2$-pretreated Cu-NTA-loaded HL-60 cells. This elevated redox-cycling activity of Cu essentially reports that exposure of cells to SNAP triggered generation of oxygen radicals via one-electron reduction of molecular oxygen and subsequent Fenton chemistry leading to production of hydroxyl radicals. Our fluorescence HPLC assay of phospholipid peroxidation revealed a pronounced decrease of PnA-labelled phospholipids after exposure of $ZnCl_2$-pretreated/Cu-NTA-loaded HL-60 cells to SNAP and reflects the degree of oxidative stress incurred by these cells. Notably, the Cu chelator neocuproine was able to effectively suppress SNAP-induced redox-cycling activity in $ZnCl_2$-treated/Cu-NTA-loaded HL-60 cells. This clearly indicates that release and/or loosening of MT-bound Cu was responsible for the enhanced redox-cycling activity in the cells. It is likely that both free Cu as well as Cu loosely bound to MTs contributed to this SNAP-induced Cu redox-cycling activity in the cells. The redox-cycling activity of Cu loosely bound to MT may take on special significance regarding the intracellular locations of Cu-mediated oxidative stress since MT can differentially localize to the cytoplasm and/or to the nucleus [45,46]. It should be noted that the time course of NO release from SNAP in the presence of $ZnCl_2$-treated and $ZnCl_2$-treated/Cu-NTA-loaded HL-60 cells was identical, as shown by our fluorescence measurements of NO with DAF-2. This suggests that participation of Cu released from MT in the catalytic decomposition of SNAP was not likely to occur.

NO is known to act as a powerful radical scavenger and very effective antioxidant preventing lipid peroxidation [47]. In addition, NO has been reported to interact with active SH groups on caspases and, thus, inhibit the execution of apoptosis [48]. The ability of SNAP to induce phospholipid peroxidation in $ZnCl_2$-pretreated/Cu-NTA-loaded HL-60 cells indicates that NO-induced release of Cu and its catalytic redox-cycling activity overwhelmed antioxidant capacity of NO as an antioxidant. Furthermore, the concentration of SNAP employed here did not generate NO in sufficient amounts to inhibit caspase activation. Thus high redox-cycling activity of Cu and resultant oxidative stress are, most probably, responsible for SNAP-induced apoptosis in HL-60 cells. In support of this, we found that neocuproine was able to completely block SNAP-induced apoptosis in $ZnCl_2$-pretreated/Cu-NTA-loaded cells.

Overall, our results indicate that NO can reverse the protective antioxidant and anti-apoptotic roles that MTs play in cells challenged with Cu [15], in contrast to the commonly held opinion that MTs and NO both function as intracellular antioxidants [9,31,47]. At another angle, our results demonstrate that NO may act as a regulator of metal occupancy and release from MTs. In this way, metals may be delivered to other protein targets, as has been predicted from *in vitro* experiments with Zn-MTs [13,14] and suggested by a fluorescence resonance energy transport-based assay of a MT chimaera in intact cells [38]. Therefore, regulation of metal binding/release activity of MTs by NO-mediated signalling is probably an important regulatory strategy. As the diverse roles of redox processes in cell signalling are becoming more evident, involvement of MTs in oxidative/nitrosative signal-transduction pathways may represent a previously unrecognized functional role for these proteins [49].

This work was supported by grants from the American Institute of Cancer Research 97-B128, National Institutes of Health (NIH) HL-64145-01A1, NIH HL-32154, EPA STAR Grant R-827151, the National Cancer Institute Oncology Research Faculty Development Program and Magee-Womens Research Institute, the Leukemia Research Foundation and the International Neurological Science Fellowship Program (F05 NS 10669) administered by NIH/National Institute of Neurological Diseases and Stroke in collaboration with the World Health Organisation, Unit of Neuroscience, Division of Mental Health and Prevention of Substance Abuse.

REFERENCES

1 Halliwell, B. and Gutteridge, J. M. C. (1990) Role of free radicals and catalytic metal ions in human disease: an overview. Methods Enzymol. **186**, 1–85

2 Ma, Y., Cao, L., Kawabata, T. T. Y., Yang, B. B. and Okada, S. (1998) Cupric nitrilotriacetate induces oxidative DNA damage and apoptosis in human leukemia HL-60 cells. Free Radic. Biol. Med. **25**, 568–575
3 Lippard, S. J. (1999) Free copper ions in the cell? Science **284**, 748–749
4 Gutteridge, J. M. and Stocks, J. (1981) Ceruloplasmin: physiological and pathological perspectives. Crit. Rev. Clin. Lab. Sci. **14**, 257–329
5 Halliwell, B. (1988) Albumin – an important extracellular antioxidant? Biochem. Pharmacol. **37**, 569–571
6 Pufahl, R. A., Singer, C. P., Peariso, K. L., Lin, S. J., Schmidt, P. J., Fahrni, C. J., Culotta, V. C., Penner-Hahn, J. E. and O'Halloran, T. V. (1997) Metal ion chaperone function of the soluble Cu(I) receptor Atx1. Science **278**, 853–856
7 Glerum, D. M., Muroff, I., Jin, C. and Tzagoloff, A. (1997) COX15 codes for a mitochondrial protein essential for the assembly of yeast cytochrome oxidase. J. Biol. Chem. **272**, 19088–19094
8 Culotta, V. C., Klomp, L. W., Strain, J., Casareno, R. L., Krems, B. and Gitlin, J. D. (1997) The copper chaperone for superoxide dismutase. J. Biol. Chem. **272**, 23469–23472
9 Lazo, J. S., Kuo, S. M., Woo, E. S. and Pitt, B. R. (1998) The protein thiol metallothionein as an antioxidant and protectant against antineoplastic drug. Chem. Biol. Interact. **111–112**, 255–262
10 Fabisiak, J. P., Tyurin, V. A., Tyurina, Y. Y., Borisenko, G. G., Korotaeva, A., Pitt, B. R., Lazo, J. S. and Kagan, V. E. (1999) Redox regulation of copper-metallothionein. Arch. Biochem. Biophys. **363**, 171–181
11 Misra, R. R., Hochadel, J. F., Smith, G. T., Cook, J. C., Waalkes, M. P. and Wink, D. A. (1996) Evidence that nitric oxide enhances cadmium toxicity by displacing the metal from metallothionein. Chem. Res. Toxicol. **9**, 326–332
12 Jacob, C., Maret, W. and Vallee, B. L. (1998) Control of zinc transfer between thionein, metallothionein, and zinc proteins. Proc. Natl. Acad. Sci. U.S.A. **95**, 3489–3494
13 Jiang, L. J., Maret, W. and Vallee, B. L. (1998) The glutathione redox couple modulates zinc transfer from metallothionein to zinc-depleted sorbitol dehydrogenase. Proc. Natl. Acad. Sci. U.S.A. **95**, 3483–3488
14 Maret, W. and Vallee, B. L. (1998) Thiolate ligands in metallothionein confer redox activity on zinc clusters. Proc. Natl. Acad. Sci. U.S.A. **31**, 3478–3482
15 Kawai, K., Liu, S. X., Tyurin, V. A., Tyurina, Y. Y., Borisenko, B. B., Fabisiak, J. P., Pitt, B. R. and Kagan, V. E. (2000) Antioxidant and anti-apoptotic function of metallothioneins in HL-60 cells challenged with copper-nitrilotriacetate. Chem. Res. Toxicol. **13**, 1275–1287
16 Fabisiak, J. P., Pearce, L. L., Borisenko, G. G., Tyurina, Y. Y., Tyurin, V. A., Razzack, J., Lazo, J. S., Pitt, B. R. and Kagan, V. E. (1999) Bifunctional anti-/prooxidant potential of metallothionein: redox signaling of copper binding and release. Antiox. Redox Signal. **1**, 309–324
17 Liu, S. X., Fabisiak, J. P., Tyurin, V. A., Borisenko, B. B., Pitt, B. R., Lazo, J. S. and Kagan, V. E. (2000) Reconstitution of apo-superoxide dismutase by nitric oxide-induced copper transfer from metallothionein. Chem. Res. Toxicol. **13**, 922–931
18 Toyokuni, S., Tanaka, T., Nishiyama, Y., Okamoto, K., Nakashima, Y., Hamazaki, S., Okada, S. and Hiai, H. (1996) Induction of renal cell carcinoma in male Wistar rats treated with cupric nitrilotriacetate. Lab. Invest. **75**, 239–248
19 Fabisiak, J. P., Kagan, V. E., Ritov, V. B., Johnson, D. E. and Lazo, J. S. (1997) Bcl-2 inhibits selective oxidation and externalization of phosphatidylserine during paraquat-induced apoptosis. Am. J. Physiol. Cell Physiol. **272**, C675–C684
20 Fabisiak, J. P., Tyurina, Y. Y., Tyurin, V. A., Lazo, J. S. and Kagan, V. E. (1998) Random versus selective membrane oxidation in apoptosis: role of phosphatidylserine. Biochemistry **37**, 13781–13790
21 Yang, J., Liu, X., Bhalla, K., Kim, C. N., Ibrado, A. M., Cai, J., Peng, T. I., Jones, D. P. and Wang, X. (1997) Prevention of apoptosis by Bcl-2: release of cytochrome c from mitochondria blocked. Science **275**, 1129–1132
22 Garrett, S. H., Somji, S., Todd, J. H. and Sens, S. A. (1998) Exposure of human proximal kidney tubule cells to Cd^{2+}, Zn^{2+}, and Cu^{2+} induces metallothionein protein accumulation but not metallothionein isoform 2 mRNA. Environ. Health Perspectives **106**, 587–595
23 Kojima, H., Nakatsubo, N., Kikuchi, K., Kawahara, S., Kirino, Y., Nagoshi, H., Hirata, Y. and Nagano, T. (1998) Detection and imaging of nitric oxide with novel fluorescent indicators: diaminofluoresceins. Anal. Chem. **70**, 2446–2453
24 Cook, J. A., Kim, S. Y., Teague, D., Krishna, M. C., Pacelli, R., Mitchell, J. B., Vodovotz, Y., Nims, R. W., Christodoulou, D., Miles, A. M. et al. (1996) Convenient colorimetric and fluorometric assays for S-nitrosothiols. Anal. Biochem. **238**, 150–158
25 Chen, P., Onana, P., Shaw, 3rd, C. F. and Petering, D. H. (1996) Characterization of calf liver Cu,Zn-metallothionein: naturally variable Cu and Zn stoichiometries. Biochem. J. **317**, 389–394
26 Kagan, V. E., Ritov, V. B., Tyurina, Y. Y. and Tyurin, V. A. (1998) Sensitive and specific fluorescent probing of oxidative stress in different classes of membrane phospholipids in live cells using metabolically integrated cis-parinaric acid. Methods Mol. Biol. **108**, 71–87
27 Folch, J., Lees, M. and Sloane-Stanley, G. H. (1957) A simple method for the isolation and purification of total lipids from animal tissues. J. Biol. Chem. **226**, 497–509
28 Chalvardjian, A. and Rudnicki, E. (1970) Determination of lipid phosphorous in nanomolar range. Anal. Biochem. **36**, 225–226
29 Reed, J. C. (1997) Cytochrome c: can't live with it – can't live without it. Cell **9**, 559–562
30 Thornberry, N. A., Rano, T. A., Peterson, E. P., Rasper, D. M., Timkey, T., Garcia-Cavo, M., Houtzager, V. M., Nordstrom, P. A., Roy, S., Vaillancourt, J. P. et al. (1997) A combinatorial approach defines specificities of members of the caspase family and granzyme B. Functional relationships established for key mediators of apoptosis. J. Biol. Chem. **272**, 17907–17911
31 Villa, P., Kaufmann, S. H. and Earnshaw, W. C. (1997) Caspases and caspase inhibitors. Trends Biochem. Sci. **22**, 388–393
32 Percival, M. D., Ouellet, M., Campagnolo, C., Claveau, D. and Li, C. (1999) Inhibition of cathepsin K by nitric oxide donors: evidence for the formation of mixed disulfides and a sulfenic acid. Biochemistry **38**, 13574–13583
33 Mallis, R. J. and Thomas, J. A. (2000) Effect of S-nitrosothiols on cellular glutathione and reactive protein sulfhydryls. Arch. Biochem. Biophys. **383**, 60–69
34 Nielson, K. B., Atkin, C. L. and Winge, D. R. (1985) Distinct metal-binding configurations metallothionein. J. Biol. Chem. **260**, 5342–5350
35 Stillman, M. J., Cai, W. and Zelazowski, A. J. (1987) Cadmium binding to metallothioneins. Domain specificity in reactions of alpha and beta fragments, apometallothionein, and zinc metallothionein with Cd^{2+}. J. Biol. Chem. **262**, 4538–4548
36 Chen, P., Munoz, A., Nettesheim, D. and Shaw, Jr., C. F. (1996) Stoichiometry and cluster specificity of copper binding to metallothionein: homogeneous metal clusters. Biochem. J. **317**, 395–402
37 Aravindakumar, C. T., Ceulemans, J. and Deley, M. (1999) Nitric oxide induces Zn^{2+} release from metallothionein by destroying zinic-sulphur clusters without concomitant formation of S-nitrosothiol. Biochem. J. **344**, 253–258
38 Pearce, L. L., Gandley, R. E., Han, W., Wasserloos, K., Kanai, A. J., McLaughlin, M. K., Pitt, B. R. and Levitan, E. S. (2000) Role of metallothionein in nitric oxide signaling as revealed by a green fluorescent fusion protein. Proc. Natl. Acad. Sci. U.S.A. **97**, 477–482
39 Stubauer, G., Giuffre, A. and Sarti, P. (1999) Mechanism of S-nitrosothiol formation and degradation mediated by copper ions. J. Biol. Chem. **274**, 28128–28133
40 Gordge, M. P., Meyer, D. J., Hothersall, J., Neild, G. H., Payne, N. N. and Noronha-Dutra, A. (1995) Copper chelation-induced reduction of the biological activity of S-nitrosothiols. Br. J. Pharmacol. **114**, 1083–1089
41 Aravindakumar, C. T., Ceulemans, J. and De Ley, M. (2000) Steric effect and effect of metal coordination on the reactivity of nitric oxide with cysteine-containing proteins under anaerobic conditions. Biophys. Chem. **85**, 1–6
42 Quesada, A. R., Byrnes, R. W., Krezoski, S. O. and Petering, D. H. (1996) Direct reaction of H_2O_2 with sulfhydryl groups in HL-60 cells: Zn-metallothionein and other sites. Arch. Biochem. Biophys. **334**, 241–250
43 Fernando, M. R., Nanri, H., Yoshitake, S., Nagata-Kuno, K. and Minakami, S. (1992) Thioredoxin regenerates proteins inactivated by oxidative stress in endothelial cells. Eur. J. Biochem. **209**, 917–922
44 Graviana, S. A. and Mieyal, J. J. (1993) Thioltransferase is a specific glutathionyl mixed disulfide oxidoreductase. Biochemistry **32**, 3368–3376
45 Woo, E. S., Dellapiazza, D., Wang, A. S. and Lazo, J. S. (2000) Energy-dependent nuclear binding dictates metallothionein localization. J. Cell Physiol. **182**, 69–76
46 Cherian, M. G. and Apostolova, M. D. (2000) Nuclear localization of metallothionein during cell proliferation and differentiation. Cell Mol. Biol. **46**, 347–356
47 Fabisiak, J. P., Tyurin, V. A., Tyurina, Y. Y., Sedlov, A., Lazo, J. S. and Kagan, V. E. (2000) Nitric oxide dissociates lipid oxidation from apoptosis and phosphatidylserine externalization during oxidative stress. Biochemistry **39**, 127–138
48 Dimmeler, S., Haendeler, J., Nehls, M. and Zeiher, A. M. (1997) Suppression of apoptosis by nitric oxide via inhibition of interleukin-1 beta-converting enzyme (ICE)-like and cysteine protease protein (CPP)-32-like proteases. J. Exp. Med. **185**, 601–607
49 Palmiter, R. D. (1998) The elusive function of metallothioneins. Proc. Natl. Acad. Sci. U.S.A. **95**, 8428–8430

Received 31 August 2000/15 November 2000; accepted 20 December 2000